Available online at www.sciencedirect.com
ScienceDirect
Earth and Planetary Science Letters 00 (2012) 1–??
Journal Logo

The onset of the lunar cataclysm as recorded in its ancient crater populations

Simone Marchi[a,b], William F. Bottke[b], David A. Kring[c], Alessandro Morbidelli[a]

[a]*Departement Cassiopée: Universite de Nice - Sophia Antipolis, Observatoire de la Côte d'Azur, CNRS*
[b]*Center for Lunar Origin and Evolution, SwRI, Boulder, Colorado, USA*
[c]*Center for Lunar Science & Exploration, USRA - Lunar and Planetary Institute, Houston, TX, USA*

1. On-line material

1.1. Crater obliteration

A number of processes are responsible for crater obliteration. Some are connected to endogenous processes, like burial by lava flows. Others are connected directly to the impactor flux, like the superposition of craters, ejecta burial and regional regolith seismic jolting. In this paper, endogenous processes are not important because we carefully excluded volcanic maria plains from the terrains under study. The process of crater obliteration due to the impact process is very complex since it relays on the target surface properties (e.g., regolith depth, particle size distribution, etc.) and the outcome of cratering events (e.g., mass and velocity of ejecta, etc). Therefore, the details of the crater obliteration process by ejecta burial are difficult to be summarized into a simple relationship, since the obliteration efficiency also depends on the degradation degree of the pre-existing craters.

In this section we deal with crater burial by ejecta blankets from a nearby basin. This process is important in order to define the terrain boundaries for crater count. Several attempts to derive scaling laws for the ejecta blanket thickness have been performed (McGetchin 1973; Pike 1974, Housen et al 1983). Here we used Eq. (1) of Kring 1995 (which is an updated version of McGetchin et al's equation), further corrected for the lunar curvature. The formula reads:

$$t(r) = 0.14 \cdot r_c^{0.74} \left(\frac{r}{r_c}\right)^{-3} \cdot \left(\frac{r/R_m}{\sin\left(r/R_m\right)}\right) \quad (1)$$

where, t is the ejecta thickness, r_c is the radius of a complex crater, R_m is the lunar radius, and r is the range from crater center ($r > r_c$). Dimensions are in meters. Note that the correction for lunar curvature is derived from simple

geometrical arguments, thus equation 1 may not be accurate at large distances from the impact point. In Figure 1, the ejecta thickness computed for several basins of interest in this work are reported. Note also that the depth of a crater increases with increasing size, therefore the burial become less effective for larger craters. As a reference value, the depth of craters ≥15 km is at least 2 km (Pike, 1977). This sets a lower limit for the ejecta thickness needed to bury pre-existing un-degraded craters.

The recent observation of the distribution of $D > 20$ km craters around Orientale basin (Head et al., 2010) shows that the formation of this basin destroyed some of large pre-existing nearby craters up to about two radii from basin center. Given Orientale's predicted ejecta thickness (about 2 km at the rims and 300 m at two radii from basin center, see Fig. 1), it is likely that the observed obliteration of craters was due to a combination of ejecta burial and seismic effects (Schultz and Gault 1975).

1.2. Al-Khwarizmi King region

The work of Head et al. (2010) shows that the highest density of $D > 20$ km craters is of the order of 0.28 km^{-4}, thereby exceeding what we measured on PNT. Their work also shows that other Pre-Nectarian terrains have higher crater densities than PNT.

Here we show an example of this, namely the Al-Khwarizmi King basin terrain (AKKT) as defined by Wilhelms (1987). This region is small enough that the $D > 70 - 80$ km crater counts are limited. In addition, the texture of the terrain is very complex, possibly a byproduct of its high crater density, and thus it is possible that some $D \sim 15-20$ km craters were missed from our counts.

Despite these limitations, we find it remarkable that the shape of AKKT crater SFDs is in general overall agreement with PNT. In particular, AKKT seems to have the same two-sloped distribution as described in the main text for NBT, SPAT, and PNT. Interestingly, the AKKT crater density is actually higher than PNT, showing that the latter is not saturated. It also seems unlikely that the observed difference could be due to statistical fluctuation around saturation, since none of these terrains contain recent and large craters.

The result above is in agreement with our crater formation/evolution code. The simulation reported in the main text demonstrates that AKKT is not saturated using model parameters of $f = 9$ and $k = 1$ (see main text for definitions). Here we show an additional simulation that assumes the ejecta blankets from craters would produce additional crater erasure. Figure 2 shows how our model is affected using $k = 1.5$ (and $f = 9$), the former set according to the extrapolation of crater obliteration derived from Orientale basin (Head et al., 2010). Even though this value probably overestimates the actual value of the k parameter, AKKT only barely reaches saturation. We speculate that perhaps this is close to the true value of k for these kinds of terrains.

References

Head, J. W., Fassett, C. I., Kadish, S. J., Smith, D. E., Zuber, M. T., Neumann, G. A., & Mazarico, E. *Science* **329**, 1504 (2010).

Housen, K. R., Schmidt, R. M., & Holsapple, K. A. *JGR* **88**, 2485 (1983).

Kring, D. A. *JGR* **100**, 16979 (1995).

McGetchin, T. R., Settle, M., & Head, J. W. *Earth and Planetary Science Letters* **20**, 226 (1973).

Pike, R. J. *JGR* **1**, 291 (1974).

Schultz, P. H., & Gault, D. E. *Moon* **12**, 159 (1975).

Wilhelms, D. E. (1987) *The Geologic History of the Moon.* (U.S. Geol. Surv. Prof. Pap. 1348, 1987).

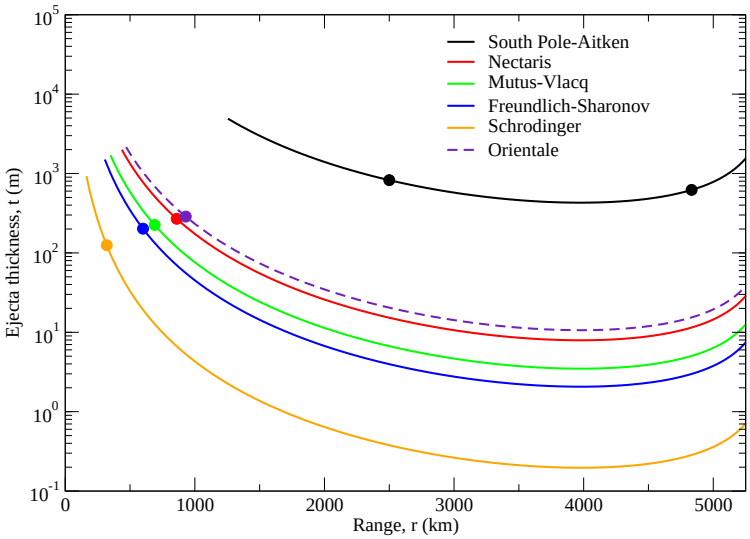

Figure 1. Ejecta blanket thickness for various basins versus range from basin's center. Dots highlight the ejecta thickness for range equal to the main topographic basin's diameters (i.e. two basin radii apart from basin center). The effect of the antipodal focusing (due to a local decrease of the deposition area on a spherical body) is clearly visible. Given the relatively large thickness of SPA basin, an additional dot at a range equal to one half of basin diameter from the antipode is reported.

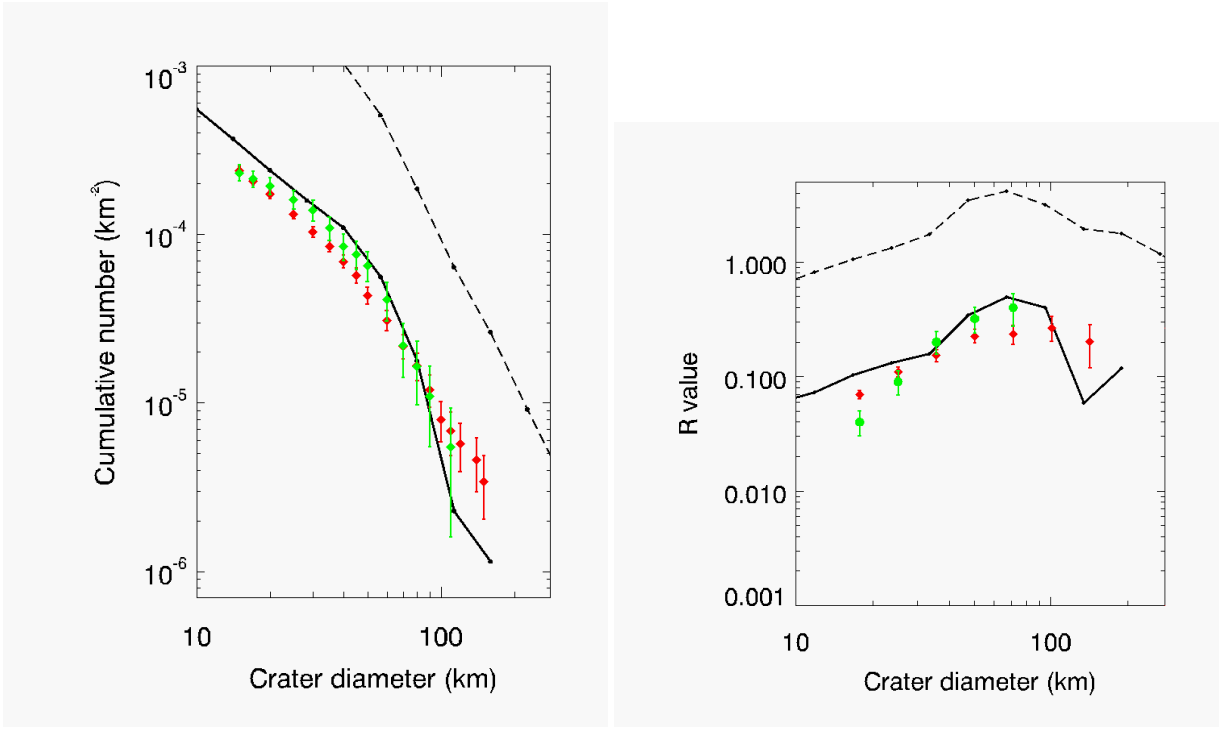

Figure 2. The plot report the crater SFDs for PNT and AKKT regions. Lines show the results of our crater terrains evolution code, for $f = 9$ and $k = 1.5$. The dashed lines indicated the production population, while the solid curves correspond to the population of crater left on the surface once the saturation has been reached.

Table 1. NBT2 crater cumulative numbers.

Diameter (km)	Cumulative Number (km^{-2})	Error (km^{-2})
15	1.24e-04	1.29e-05
17	1.06e-04	1.20e-05
20	9.17e-05	1.11e-05
25	7.01e-05	9.72e-06
30	5.66e-05	8.74e-06
35	4.72e-05	7.98e-06
40	3.64e-05	7.01e-06
45	3.23e-05	6.61e-06
50	2.56e-05	5.88e-06
60	2.29e-05	5.56e-06
70	1.75e-05	4.86e-06
80	1.08e-05	3.81e-06
90	8.10e-06	3.30e-06
100	5.39e-06	2.70e-06
110	2.70e-06	1.91e-06
130	1.35e-06	1.35e-06

Table 2. SPAT2 crater cumulative numbers.

Diameter (km)	Cumulative Number (km^{-2})	Error (km^{-2})
15	1.79e-04	8.61e-06
17	1.61e-04	8.16e-06
20	1.36e-04	7.52e-06
25	1.04e-04	6.58e-06
30	8.33e-05	5.87e-06
35	7.13e-05	5.43e-06
40	5.93e-05	4.95e-06
45	4.97e-05	4.54e-06
50	4.35e-05	4.25e-06
60	3.27e-05	3.68e-06
70	2.28e-05	3.07e-06
80	1.86e-05	2.78e-06
90	1.49e-05	2.49e-06
100	9.53e-06	1.99e-06
110	7.04e-06	1.71e-06
120	5.39e-06	1.49e-06
130	4.56e-06	1.37e-06
140	3.73e-06	1.24e-06
150	2.90e-06	1.10e-06
170	2.49e-06	1.01e-06
200	1.66e-06	8.29e-07
300	1.24e-06	7.18e-07
450	4.14e-07	4.14e-07

Table 3. PNT2 crater cumulative numbers.

Diameter (km)	Cumulative Number (km^{-2})	Error (km^{-2})
15	2.40e-04	1.17e-05
17	2.07e-04	1.09e-05
20	1.73e-04	9.95e-06
25	1.32e-04	8.69e-06
30	1.03e-04	7.69e-06
35	8.52e-05	6.98e-06
40	6.92e-05	6.29e-06
45	5.72e-05	5.72e-06
50	4.35e-05	4.98e-06
60	3.09e-05	4.20e-06
70	2.17e-05	3.52e-06
80	1.66e-05	3.08e-06
90	1.20e-05	2.62e-06
100	8.01e-06	2.14e-06
110	6.86e-06	1.98e-06
120	5.72e-06	1.81e-06
140	4.57e-06	1.62e-06
150	3.43e-06	1.40e-06
300	2.29e-06	1.14e-06
350	1.71e-06	9.90e-07
450	1.14e-06	8.09e-07
600	5.72e-07	5.72e-07